Physica E 166 (2025) 116134

Contents lists available at ScienceDirect

Physica E: Low-dimensional Systems and Nanostructures

journal homepage: www.elsevier.com/locate/physe

Giant excitonic magneto-Stark effect in wide GaAs/AlGaAs quantum wells

D.K. Loginov *, I.V. Ignatiev

Spin Optics Laboratory, St. Petersburg State University, Ulyanovskaya 1, Petrodvorets, 198504, St. Petersburg, Russia

ARTICLE INFO

Editor: Ming-Wei Wu

Keywords:
Magneto-Stark effect
Exciton
Magnetic field
Quantum well

ABSTRACT

We have studied the magneto-Stark effect of exciton states with large wave vectors, significantly exceeding the wave vector of light. This magneto-Stark effect can be called "giant" in comparison with a similar effect observed in bulk materials in comparable magnetic fields. In this work, we propose a microscopic model of the "giant" magneto-Stark effect. The model does not contain any free parameters. The numerical results obtained in the framework of this model quantitatively describe the experimental results published earlier in Ref. S. Y. Bodnar et al., (2017) for a heterostructure with a wide GaAs/AlGaAs quantum well in a magnetic field.

Introduction

Optical spectroscopy of wide quantum wells (QWs) provides rich information on the states of moving excitons [1–3]. A QW is considered wide in the case when its thickness exceeds the exciton Bohr radius by one order of magnitude [4,5]. In wide QWs, the exciton center-of-mass motion is quantized as it is experimentally and theoretically confirmed for the GaAs/$Al_xGa_{1-x}As$ QWs [6–13], for the ZnSe/ZnS_xSe_{1-x} QWs [14], for the $In_xGa_{1-x}As$/GaAs [15], and for the PbI_2 thin films [16]. The quantization of the exciton motion results in the appearance of discrete energy levels, which manifest themselves as resonances in optical spectra.

Experimental and theoretical studies of the quantization of exciton motion in different external magnetic and electric fields, as well as the strain field, are of particular interest. Application of external fields often leads to new effects, which allows one to deeply understand the nature and properties of exciton states. For example, an uniaxial stress applied to a wide QW induces the convergence of heavy and light exciton masses and leads to the phase inversion of the exciton resonances in optical spectra [17,18]. An external electric field results in modification of the electron–hole relative motion in the exciton, in a decrease of the exciton–light coupling, and in changes of the exciton dispersion described by the linear-in-wave vector terms in the exciton Hamiltonian [19,20].

An external magnetic field is another example of a field inducing a variety of effects in the exciton system [21–36]. Two geometries of experiments with magnetic fields are typically considered. In Faraday geometry, when the magnetic field is parallel to the exciton wave vector, several effects have been observed. One of them is the exciton spin splitting, whose value depends on the exciton wave vector. In optical spectra, this effect manifests itself as the dependence of the Zeeman splitting on the QW thickness, see, e.g., Refs. [21–28,36]. For the case of wide QWs, this effect is treated as the dependence of the g-factor on the number of the exciton quantum-confined state [23,24,28].

In the Voigt geometry, the magnetic field is directed perpendicular to the wave vector of exciton. In this case, the magnetic field leads to a modification of exciton dispersion that is the dependence of the exciton energy on its wave vector. This effect is explained in terms of an increase in exciton mass [29–31,33–35] or an exciton diamagnetic shift, which is dependent on the exciton wave vector [32].

In this work, we theoretically study the quantum-confined exciton states in a wide GaAs/$Al_{0.3}Ga_{0.7}As$ QW in a transverse magnetic field (Voigt geometry). We consider the influence of a magnetic field on the moving exciton as an impact of an effective electric field. This electric field results in an exciton energy shift because of the Stark effect. For excitons moving across a magnetic field, this effect is extensively discussed in the literature for bulk semiconductors, see, e.g., Refs. [37–47], as well as for double quantum wells and stacking faults, see Refs. [48–50], and it is called the magneto-Stark effect (MSE). However, in those cases, it was possible to observe only the exciton states for which the wave vector is equal to the wave vector of light. This restricts the strength of the effective electric field and, consequently, the magnitude of MSE.

We propose a model of MSE in a wide QW, the spectroscopy of which allows to observe the states of quantization of the exciton center-of-mass motion. The wave vectors of these exciton states significantly exceed the wave vector of light. Therefore, the MSE is also much stronger than the similar effect for bulk semiconductors. Such a "giant" MSE in a wide QW has been experimentally observed, in particular, in the works [31,32,34]. In the work [34], exciton reflectance spectra

* Corresponding author.
E-mail address: loginov999@gmail.com (D.K. Loginov).

https://doi.org/10.1016/j.physe.2024.116134
Received 31 July 2024; Received in revised form 25 September 2024; Accepted 22 October 2024
Available online 31 October 2024
1386-9477/© 2024 Elsevier B.V. All rights are reserved, including those for text and data mining, AI training, and similar technologies.

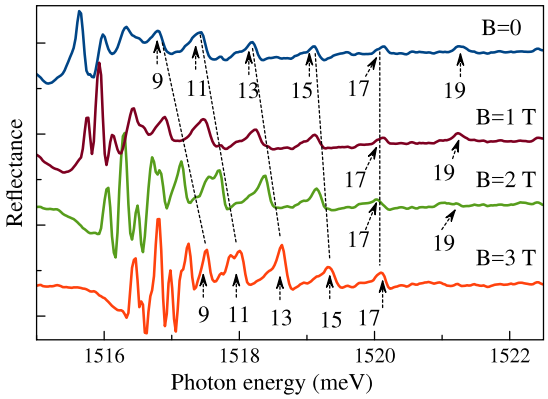

Fig. 1. Experimental reflection spectra of a heterostructure with the 225-nm GaAs QW at $B = 0$, 1, 2, and 3 T. Numbers $N = 9, 11, \ldots, 19$ indicate the energy levels corresponding to the quantization of the exciton motion. The dotted lines show the approximate position of the reflection oscillation maxima. The experimental data are adopted from Ref. [34].

of a heterostructure containing a 225-nm GaAs/$Al_{0.3}Ga_{0.7}As$ QW were measured in magnetic fields B from 0 to 3 T applied to the structure in the Voigt geometry. Several typical spectra are shown in Fig. 1.

The spectra exhibit a dominant amplitude feature corresponding to the main optical transition of the heavy-hole exciton, for which the wave vector is $K = q$, where q is the wave vector of light. Higher in energy, low-amplitude reflectance oscillations are observed, which are related to the quantization of the center-of-mass exciton motion. In Ref. [34], each oscillation was associated with the number N of the exciton quantization level. In zero field, the energy of oscillation maxima (exciton resonances) increases quadratically with increasing N, in accordance with the model of the center-of-mass quantization of exciton in a wide QW [1–16]. An exciton wave vector K can be introduced, which takes discrete values at the exciton resonances,

$$K_N = \frac{\pi N}{L_{QW} - 2L_D}, \tag{1}$$

where L_{QW} is the thickness of the well layer and $L_D \approx 15$ nm is the value of the so-called "dead layer" [6,34].

In the presence of a magnetic field, the energy of these oscillations increases because of the exciton diamagnetic shift [34]. However, the larger the oscillation number N, the smaller the increase in energy. This effect is observed as a convergence of spectral oscillations with increasing field, see Fig. 1. Here we prove that this phenomenon is caused by MSE. Namely, we show that the larger the product $K_N B$, the larger exciton energy change induced by MSE. Together with the diamagnetic shift of the exciton states to the higher energies, which is independent on N, the MSE results in slowing down the energy shift with N that is in convergence of spectral oscillations observed experimentally.

We also consider whether there are other mechanisms, in addition to MSE, that lead to an N-dependent exciton energy decrease in the magnetic field. To solve these theoretical problems, a microscopic model is proposed that does not contain any free parameters. In the framework of the model, the energies and wave functions of the exciton in a magnetic field in a QW are calculated.

The paper is organized as follows. Section 1 is devoted to consideration of the exciton Hamiltonian in an external magnetic field applied in the Voigt geometry. In Section 2, we perform theoretical calculations of exciton energies, which are compared with those obtained from the experimental reflectance spectra. A short discussion of the obtained results and conclusion is given in Section 3.

1. Basic equations for exciton in magnetic field

Let us consider an exciton in a bulk crystal of the zinc-blende symmetry moving along the axis, which coincides with the [001] crystal axis. In this case, the projection of the exciton wave vector on the axis is K. The magnetic field $\mathbf{B}$ is directed along the x axis, that is, $B = B_x$, $B_y = B_z = 0$. The coordinate axis x is directed along the crystal axis [100].

Exciton states in GaAs-type materials are formed by electron states of the twofold degenerate conduction band Γ_6 and hole states of the fourfold degenerated valence band Γ_8. The conduction band states differ in their electron spin projections, $s_e = \pm 1/2$, and the valence band states differ in their projections of the total angular momentum of the hole, $j_h = \pm 3/2, \pm 1/2$. There are eight exciton states in total, $|j_h, s_e\rangle$, differing in configurations of spin projections of electrons and holes.

The exciton Hamiltonian is the sum of the Hamiltonians of free electrons and holes, $\hat{\mathrm{H}}_c$ and $\hat{\mathrm{H}}_v$, and their Coulomb interaction,

$$\hat{\mathrm{H}}_{\mathrm{X}} = \hat{\mathrm{H}}_c + \hat{\mathrm{H}}_v - \frac{e^2}{\varepsilon_0 r}. \tag{2}$$

Here e is the electron charge, ε_0 is the background dielectric constant of the semiconductor, and $r = |\mathbf{r}_e - \mathbf{r}_h|$ is the distance between the electron and the hole, where $\mathbf{r}_e$, $\mathbf{r}_h$ are the radius-vectors of the electron and the hole.

This Hamiltonian can be written in terms of the momentum operators of the relative motion of the electron and the hole in the exciton, $\hat{p}_\alpha$, and the wave vector of the exciton center-of-mass motion, K, see e.g., Refs. [1,3,51]. The first operator has the form $\hat{p}_\alpha = -i\hbar\partial/\partial\alpha$, where $\alpha = x, y, z$ are the coordinates of the relative electron–hole motion. The wave vector of the exciton center-of-mass motion can be considered simply as a number.

The magnetic field is taken into account in the exciton Hamiltonian through the terms dependent on the vector potential $\mathbf{A}$. The components of the vector potential in the Landau gauge are, see, e.g., Ref. [52]

$$A_z = By, \text{ and } A_x = A_y = 0. \tag{3}$$

As a result, the matrix operator of the Hamiltonian (2) can be written as (see Appendix A)

$$\begin{aligned}\hat{\mathbb{H}}_X = {} & \mathbb{L}\frac{\hbar^2 K^2}{2} - \frac{\hat{p}^2}{2\mu} - \frac{e^2}{\varepsilon_0 r} + \left(\frac{e}{c}\right)\mathbb{L}\hbar K B y \\ & - 2\frac{\gamma_3}{m_0}\left(\frac{e}{c}\right)\frac{m_e m_h}{(m_e+m_h)^2}\{J_y, J_z\} K B y \\ & + \left(\frac{e}{c}\right)^2 \frac{m_e^3 + m_h^3}{2(m_e+m_h)^2 m_e m_h} B^2 y^2.\end{aligned} \tag{4}$$

Here the first term is the kinetic energy of the exciton center-of-mass motion. In the matrix of reciprocal exciton masses $\mathbb{L}$, all off-diagonal elements are zero and the diagonal elements are $1/M_{h(l)}$. Here, $M_{h(l)} = m_e + m_{hh(lh)}$ are the masses of heavy-hole (index h) and light-hole (index l) excitons, where m_e is the effective mass of the electron and $m_{hh(lh)}$ are the masses of heavy (hh) or light (lh) holes. In the approximation of large wave vectors ($K \gg 1/a_B$, where a_B is the exciton Bohr radius), the masses of the heavy and light holes are assumed to be equal to $m_{hh(lh)} = m_0/(\gamma_1 \pm 2\gamma_2)$, where γ_1 and γ_2 are the Luttinger parameters and m_0 is the mass of a free electron [53]. Note that the MSE could be, in principle, discussed for states with small wave vectors K. The main problem in this case consists in the non-parabolicity of dependence of the exciton energy on K (see Ref. [53]) that strongly complicates the modeling of the MSE at small K. On the other hand, experimental information about the exciton states with small K is limited because these states overlap each other in wide QWs and they are not observable in bulk crystals. Therefore, in the following, we only consider exciton states with large wave vectors.

The second term in Eq. (4) describes the kinetic energy of the relative motion of the electron and hole in the exciton. It contains the

reduced mass, $\mu = m_e m_h/(m_e + m_h)$, where $m_h = m_0/\gamma_1$, see [53]. The quantity $\hat{p}^2 = \hat{p}_x^2 + \hat{p}_y^2 + \hat{p}_z^2$ is the squared momentum operator of relative motion.

The fourth and fifth terms in Eq. (4) contain both the wave vector of the exciton center-of-mass motion and the coordinate of the relative electron–hole motion. These are the key terms for the MSE as we show in the next section. The constant c is the speed of light. The fifth term comes from the anisotropic part of the hole Hamiltonian [54]. Quantity γ_3 is the Luttinger parameter. The matrix operator $\{J_y, J_z\}$ describes the mixing of states of the heavy-hole excitons $|\pm 3/2, s_e\rangle$ with those of the light-hole excitons $|\pm 1/2, s_e\rangle$. Here, J_y and J_z are the hole angular momentum matrices.

The last term in Eq. (4) describes the exciton diamagnetic shift. A theoretical model of the diamagnetic shift in relatively narrow QWs is, in principle, a nontrivial problem. Besides the last term in (4), several effects, such as the heavy-hole–light-hole exciton coupling, the coupling of the heavy-hole exciton states with the states of the spin–orbit split-off band, and the effects at the QW/barrier interfaces, can contribute to the diamagnetic shift. An analysis performed in Ref. [36] has shown that all these contributions are really important for the narrow QWs. However, in the case of the wide QWs considered in this work, the relative electron–hole motion is weakly affected by the QW interfaces, as it is extensively discussed in many papers, see [4,5]. Therefore, the diamagnetic shift in wide QWs should be similar to that in bulk crystal. All the contributions discussed in Ref. [36] should be negligibly small in bulk GaAs. This conclusion has been verified in many publications (see, e.g., [55–57]). Our analysis of the experiment of Ref. [34] performed below also confirms this conclusion. Therefore, these effects are not discussed below in the paper.

The expression (4) should also contain a term describing the exciton Zeeman splitting, $\mu_B(g_e\sigma_x + J_x g_h)B$. Here σ_x is the Pauli matrix, g_e and g_h are the electron and hole g-factors, respectively, and μ_B is the Bohr magneton. However, simple estimates show that for GaAs this splitting does not exceed 0.08 meV in the magnetic field $B = 3$ T. This is due to the small value of the electron g-factor, $g = -0.44$, and the negligible small value of the transverse component of the g-factor of the heavy hole [54]. The splitting is much smaller than the energy shifts described by other terms of the expression (4). Therefore, we do not consider this term hereafter.

The assumptions described allow us to represent the exciton Hamiltonian as a block-diagonal matrix. The blocks are the matrices of size 2×2, the off-diagonal elements of which mix the states $|\pm 3/2, s_e\rangle$ with the states $|\pm 1/2, s_e\rangle$.

To further simplify the problem, we consider MSE only for the optically active states of the heavy-hole exciton, which most clearly manifest themselves in optical experiments. The light-hole exciton resonances are hardly visible in the experiments for wide QWs due to smaller oscillator strength and larger broadening [6,13,34]. At the same time, the mixing of the heavy-hole exciton states with the optically inactive light-hole exciton states should be taken into account. Finally, we should note that the behavior of the heavy-hole exciton states $|+3/2, -1/2\rangle$ and $|-3/2, +1/2\rangle$ are equivalent in the framework of the assumptions made. Therefore, it is sufficient to consider only one of them. We consider only the $|3/2, -1/2\rangle$ state, which is mixed with the optically inactive $|1/2, -1/2\rangle$ state.

2. Magneto-Stark effect for large exciton wave vectors

To calculate the energy and wave functions of the relative motion of an electron and a hole in an exciton, one should solve the eigenvalue problem with the Hamiltonian (4). It is convenient to transform a Cartesian coordinate system into a cylindrical one according to the following expressions

$$\rho = \sqrt{x^2 + z^2}, \quad y = y, \quad \phi = \arctan(x/z). \tag{5}$$

It should be emphasized that the optically active states observed experimentally correspond to the lowest state of the relative electron–hole motion. These states are symmetric in angle ϕ, and, correspondingly, they do not depend on this variable. Therefore, the Hamiltonian considered here does not contain angle ϕ and its derivatives.

In the cylindrical coordinates (5), the matrix operator of the Hamiltonian takes the form, see, e.g., Refs. [58,59]

$$\hat{\mathbb{H}}_X = \begin{pmatrix} \hat{H}_h & \hat{V}_{KB} \\ \hat{V}_{KB}^* & \hat{H}_l \end{pmatrix}, \tag{6}$$

where

$$\hat{H}_{h,l} = \frac{\hbar^2 K^2}{2M_{h,l}} - \frac{\hbar}{2\mu}\left(\frac{\partial^2}{\partial\rho^2} + \frac{1}{\rho}\frac{\partial}{\partial\rho} + \frac{\partial^2}{\partial y^2}\right) - \frac{e^2}{\varepsilon_0\sqrt{\rho^2 + y^2}} + eF_{KB}^{(h,l)} y + DB^2 y^2. \tag{7}$$

Here the following notations are introduced

$$\hat{V}_{KB} = -e\gamma_3\hbar\sqrt{3}\frac{m_e m_h}{(m_e + m_h)^2 m_0 c} KBy, \tag{8}$$

$$F_{KB}^{(h,l)} = \frac{\hbar KB}{M_{h,l}c}, \tag{9}$$

$$D = \left(\frac{e}{c}\right)^2 \frac{m_e^3 + m_h^3}{2(m_e + m_h)^2 m_e m_h}. \tag{10}$$

Note that the second term in the second line of the expression (7) can be formally represented as the energy contribution from the effective electric field, $F_{KB}^{(h,l)}$, defined by Eq. (9). It depends on the product of the exciton wave vector and the magnetic field. The energy shift described by this term has previously been discussed in the literature as the magneto-Stark effect [37–47]. Similar to the usual Stark effect, it leads to a decrease in exciton energy.

The last term in the expression (7) describes the diamagnetic shift of the exciton. The action of this term can be considered as a parabolic potential along the y coordinate, which, in addition to the Coulomb interaction, confines the motion of the electron and the hole in the exciton. The steepness of the parabolic potential depends on the square of the magnetic field. The height of the potential tends to infinity as y^2 increases when the magnetic field $B \neq 0$. This term plays an important role in the model of MSE at large K (giant MSE), since the parabolic potential does not allow the electron and the hole in the exciton to move from each other to infinity in the effective electric field.

Note that the Coulomb potential for the electron and the hole in the exciton becomes partially tunnel-transparent in the non-zero electric field, see, e.g., Refs. [60,61]. This means that the exciton dissociates if we do not take into account the diamagnetic terms in the expression (7). Consequently, exciton states do not decay in the effective electric field only owing to the effect of the diamagnetic shift of the exciton energy.

The perturbation $\hat{V}_{KB}$ defined by Eq. (8) describes the mixing of states of heavy-hole and light-hole excitons. This mixing occurs because the symmetry of the crystal lattice is lower than the spherical symmetry of three-dimensional space. In crystals with a cubic lattice, this leads to corrugation of the surface of constant hole energy because of coupling light-hole and heavy-hole states, see, e.g., [54].

The numerical solution of the eigenvalue problem for the Hamiltonian (7) is carried out using the representation of derivatives by difference schemes on a finite discrete coordinate grid [62]. Since this Hamiltonian involves second derivatives with respect to two variables as well as the mixing of heavy-hole and light-hole excitons, the problem reduces to the diagonalization of a seven-diagonal matrix, see Appendix B.

Examples of the cross sections of the wave functions of the heavy-hole exciton $|3/2, -1/2\rangle$ calculated by this way are presented in Fig. 2(a), (b). The following values of the material constants for bulk GaAs were used in the calculations: the Luttinger parameters $\gamma_1 = 6.8$, $\gamma_2 = 2.3$, and $\gamma_3 = 2.9$; the electron effective mass $m_e = 0.067\ m_0$ (see

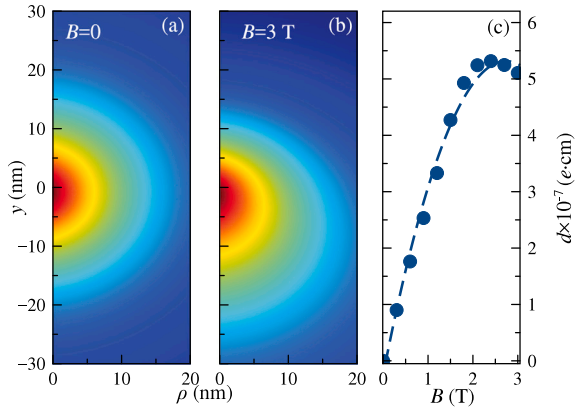

Fig. 2. Cross sections of the wave functions calculated for the exciton with the wave vector $K = 2.5 \times 10^6$ cm^{-1} in the magnetic fields $B = 0$ (a) and $B = 3$ T (b). Panel (c): dependence of dipole moment d of the exciton with wave vector $K = 2.5 \times 10^6$ cm^{-1} on the magnetic field strength. Points are the calculation results; the curve is a parabolic approximation.

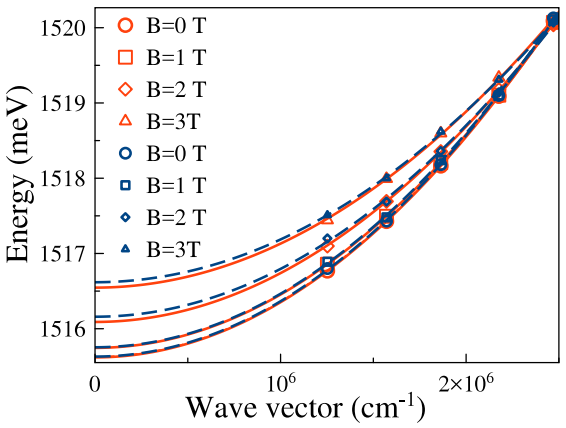

Fig. 3. Comparison of the theoretically obtained energies of the exciton states (red symbols) with energies of maxima in experimental spectra (blue symbols) in magnetic fields $B = 0$, 1, 2, and 3 T for different values of the exciton wave vector. Curves approximate the field dependence of the energies using expression (12).

Table 3.9 in Ref. [63]); the background dielectric constant $\varepsilon_0 = 12.56$ [64]. As the figure shows, the magnetic field for a moving exciton leads to some asymmetry in the wave function of the relative motion. This asymmetry is caused by the action of the effective electric field, which leads to a distortion of the Coulomb potential and, as a consequence, a shift of the maximum of the wave function from the point $\rho = 0$, $y = 0$. In other words, the effective electric field leads to exciton polarization.

The polarization can be expressed in terms of the exciton dipole moment, $d = e \cdot \langle 3/2, -1/2|y|3/2, -1/2\rangle$. The magnetic field dependence of $d(B)$ for the exciton with the wave vector $K = 2.5 \times 10^6$ cm^{-1} is shown in Fig. 2(c). As seen, in small magnetic fields $B \leq 2$ T, the dipole moment increases. This is due to the action of the effective electric field, which leads to MSE. At larger magnetic fields, $B > 2$ T, the magnitude of the dipole moment is saturated and tends to decrease. The decrease is due to the influence of the exciton diamagnetic effect, which confines the relative electron–hole motion. The confining potential is proportional to the square of the applied magnetic field. Correspondingly, for $K = 2.5 \times 10^6$ cm^{-1}, the influence of the diamagnetic shift becomes more significant than the influence of the effective electric field linearly depending on B.

To verify the numerically obtained results, we compared them with the experimental results published earlier in the paper [34]. In the absence of a magnetic field, the energy of the exciton center-of-mass quantization level can be described by the expression:

$$E(K_N, 0) = E_g + R_X + \frac{\hbar^2 K_N^2}{2M_h}, \tag{11}$$

where E_g is the band gap in the semiconductor and $R_X = -\mu e^4/(2\hbar^2\varepsilon^2)$ is the binding energy of the ground exciton state in a bulk crystal. The discrete values of the wave vector K_N are determined by the expression (1).

Knowing the energy distances between the maxima of spectral oscillations in a zero magnetic field from the experiment and the thickness of the QW, it is possible to determine the values of the wave vector K_N corresponding to the oscillations. The K_N values obtained in this way are used to calculate the energies of the corresponding exciton states in different magnetic fields. The calculation results for $B = 0$, 1, 2, and 3 T are presented in Fig. 3. This figure also shows the exciton energies obtained from the experiment in the paper [34]. As seen, the figure demonstrates good agreement between the calculations and the experimental data.

Both the experimental and calculated values of the exciton energies can be approximated by the expression:

$$E(K_N, B) = E_g + R_X + \frac{\hbar^2 K_N^2}{2M_h(B)}. \tag{12}$$

The quantity $1/M_h(B)$ is the exciton reciprocal mass, which varies in the applied field B, see [34]. Fig. 4 shows the theoretical values obtained in this work and the experimental values of $1/M_h(B)$ obtained in the work [34] for the magnetic field strength up to 3 T. We approximated the numerically obtained magnetic field dependence of the reciprocal exciton mass by the expression

$$\frac{1}{M_h(B)} = \frac{1}{M_h(0)} - \alpha B^2. \tag{13}$$

Here $1/M_h(0)$ is the reciprocal exciton mass in zero field and $\alpha = 0.046\ m_0^{-1} \times \mathrm{T}^{-2}$. In Ref. [34], a similar expression was used to fit the experimental data. The experimentally obtained value of this parameter, $\alpha = 0.048\ m_0^{-1} \times \mathrm{T}^{-2}$. So, the theory well agrees with the experiment. Note that in the calculations we employ only the material parameters of GaAs, published in literature. The good agreement between the theory and the experiment indicates that the material parameters of GaAs used in the calculations are sufficiently accurate. The agreement also indicates that all valuable effects of magnetic field on the moving exciton are included in the theory. The obtained results allow one to expect that the experimental study and theoretical modeling of MSE in other semiconductors can be used to refine material parameters if they are known with low accuracy.

Let us analyze the role of the heavy-hole–light-hole mixing of exciton states in the change of $1/M_h(B)$. First, we ignore the mixing, $\hat{V}_{KB} = 0$, but keeping MSE, $F_{KB}^{(h)} \neq 0$. The results are shown in Fig. 4. As seen, the change in the reciprocal mass in this case is significantly weaker compared to that when the mixing is included in the calculations. Moreover, the dependence $1/M_h(B)$ for $B > 0.5$ T is linear with good accuracy. Only for small $B \leq 0.5$ T, this dependence is parabolic. Thus, the mixing of the heavy-hole and light-hole exciton states leads to significant qualitative and quantitative changes in the $1/M_h(B)$ dependence.

Another case when the MSE contribution is absent ($F_{KB}^{(h)} = F_{KB}^{(l)} = 0$) but the heavy-hole–light-hole exciton coupling is present ($\hat{V}_{KB} \neq 0$) is also shown in Fig. 4. As seen $1/M_h(B)$ is almost independent of the applied magnetic field. In other words, the contributions of the MSE and mixing of heavy-hole and light-hole exciton states to the $1/M_h(B)$ dependence are not additive.

This non-additivity of the contributions is caused by the redistribution of the MSE owing to the mixing of the heavy-hole and light-hole exciton states by perturbation $\hat{V}_{KB}$. The effective electric fields for heavy-hole and light-hole excitons are shown in expression (9). In GaAs, $F_{KB}^{(l)}$ is about 3.4 times higher than $F_{KB}^{(h)}$. Therefore, without perturbation $\hat{V}_{KB}$, the MSE for the light-hole exciton should also be 3.4

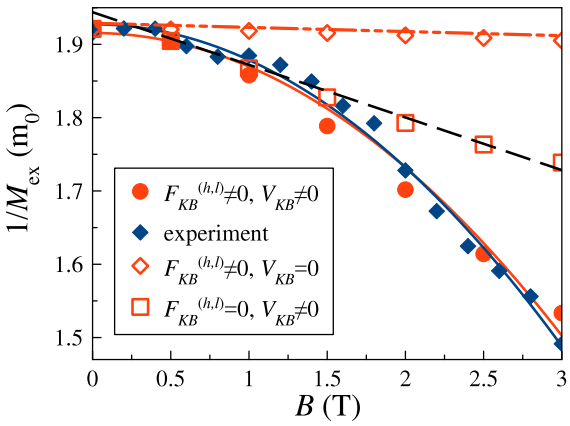

Fig. 4. Calculated (red filled circles) and obtained in Ref. [34] experimental (blue diamonds) values of the reciprocal mass of the heavy-hole exciton. Solid curves are approximations with the expression (13). The red empty squares show the calculation results for $F_{KB}^{(h,l)} \neq 0$ and $\hat{V}_{KB} = 0$ and the empty red diamonds for $\hat{V}_{KB} \neq 0$ and $F_{KB}^{(h)} = F_{KB}^{(l)} = 0$. Dashed lines are linear approximations.

times stronger than for the heavy-hole exciton. Mixing by perturbation $\hat{V}_{KB}$ in (7) leads to an effective nonlinear enhancement of the MSE for the heavy-hole exciton at the expense of weakening this effect for the light-hole exciton.

Let us compare now the magnitude of the MSE in a wide QW and in a bulk crystal. This magnitude is determined by the value of the effective electric field, which linearly depends on the exciton wave vector, see Eq. (9). In optical spectra of bulk materials, only the exciton states with a wave vector equal to the wave vector of light ($q \approx 2.7 \times 10^5 \text{cm}^{-1}$ for GaAs) are observed. The exciton states considered in this paper correspond to much larger wave vectors exceeding the wave vector of light by about an order of magnitude. For example, the maximum value of the exciton wave vector considered in this work exceeds q approximately ten times, $K \approx 2.5 \times 10^6$ cm^{-1}. The effective electric field proportionally exceeds this magnitude for the bulk GaAs. As a consequence, the MSE in wide quantum wells is giant in comparison with the effect in bulk semiconductors.

An external electric field directed against the effective field can be used to compensate for the MSE, see, e.g., Ref. [38]. However, in the case of quantum wells, where the exciton states with different wave vectors are observed, such compensation is possible only for one of the states since the effective field depends on the wave vector. It should be noted that the implementation of such experiments for large wave vectors and, accordingly, large effective electric fields is a non-trivial task because of the high conductivity along the quantum well layer, which does not allow applying an electric field of noticeable magnitude.

The exciton energy shift due to the MSE, like the usual Stark shift, partially occurs because of a decrease in the binding energy, see, e.g., [65,66]. Another origin of the shift is the interaction of the induced dipole moment of the exciton [see Fig. 2(c)] with the electric field. The energy decrease is determined by the strength of the effective electric field, which is proportional to the magnitude of the wave vector. Consequently, the binding energy decreases much stronger in quantum wells (by about one order of magnitude in our case) than in bulk materials. Still, as estimates show, the binding energy of exciton remains nonzero, which saves the exciton as the coupled electron–hole pair at all magnetic fields and wave vectors considered in this work.

The exciton in the effective electric field increases in size. In particular, it acquires a dipole moment along the electric field direction, see Fig. 2(c), and it becomes slightly larger in the perpendicular direction, see Fig. 2(b). The latter is due to the decrease of the binding energy. We should note again that the magnitude of these changes in the exciton size is proportional to the effective electric field and, therefore, considerably larger than in the case of bulk materials.

We have considered the MSE for a wide QW, in which the QW layer is described by the same material parameters as the bulk GaAs. However, this model remains applicable to wide QWs based on other semiconductors of cubic symmetry, whose properties can be described by the Luttinger Hamiltonian. The mixing of heavy-hole and light-hole exciton states originates from the off-diagonal terms of the Luttinger Hamiltonian, which describes the corrugation of the constant energy surface for holes. The corrugation strength is described by the Luttinger parameter γ_3, which is a material constant. Besides, the light-hole–heavy-hole exciton mixing depends on the ratio of the electron and the hole masses, which are included in the perturbation operator (8). So, parameter γ_3 and the ratio of masses control the mixing in different semiconductors. For the case of QWs, in which the uniaxial deformation along the growth axis occurs because of the difference of lattice constants of the QW and barrier layers, the splitting of the energy of the light-hole and heavy-hole excitons should be introduced into expression (4). This splitting does not depend on the applied magnetic field and the exciton wave vector.

3. Conclusions

The effect of a magnetic field on exciton states in wide quantum wells is analyzed in the framework of the giant magneto-Stark effect. Previously, this effect was analyzed in a similar way only for bulk materials and for stacking faults, i.e., for relatively small exciton wave vectors comparable to that light. Exciton states observed in the reflectance spectra of wide quantum wells are characterized by wave vectors that are significantly greater than the wave vector of light. Correspondingly, the magneto-Stark effect in such wells is strongly magnified in comparison with a similar effect in bulk materials.

The diamagnetic shift of the exciton energy plays an important role in the giant effective electric field, which tends to dissociate the exciton. However, diamagnetic energy shift, which quadratically increases with magnetic field, prevents the exciton from dissociating into free carriers in the effective electric field.

The analysis also shows that, in the case of the giant magneto-Stark effect the mixing of heavy-hole and light-hole excitons plays an important role. This mixing leads to a redistribution of the magneto-Stark effect strength between the states of light-hole and heavy-hole excitons. The mutual action of the magneto-Stark effect and the mixing of heavy- and light-hole states can be described as an effective reduction in the reciprocal mass of the exciton in a magnetic field.

A comparison of the calculated values for the exciton energy shifts and the effective change in the reciprocal exciton mass caused by the magneto-Stark effect demonstrates good agreement between theory and experimental results, published in Ref. [34]. This agreement is achieved by employing only the material parameters of GaAs without any fitting parameters. We believe that the good accuracy of the model could be used in MSE experiments to determine the material parameters of the poorly studied semiconductor compounds. We should note, however, that the proposed model is applicable only in the case of large exciton wave vectors significantly exceeding the wave vector of light.

CRediT authorship contribution statement

D.K. Loginov: Investigation, Formal analysis, Conceptualization. **I.V. Ignatiev:** Supervision, Conceptualization.

Declaration of competing interest

The authors declare that they have no known competing financial interests or personal relationships that could have appeared to influence the work reported in this paper.

Acknowledgment

Financial support from the Russian Science Foundation, grant No. 19-72-20039, and the St.Petersburg State University, grant No. 122040800257-5, is acknowledged.

Appendix A

Let us assume that the Cartesian coordinates x, y, and z are directed along the crystallographic directions [100], [010], and [001], respectively. Than the Hamiltonians of a free electron in the conduction band and a free hole in the degenerate valence band, which are included in the expression (2), have the form, see, e.g., [54]

$$\begin{aligned}\hat{\mathrm{H}}_c &= \frac{\hbar^2\hat{k}_e^2}{2m_e}\\ \hat{\mathrm{H}}_v &= \frac{\hbar^2}{2m_0}\left[\gamma_1\hat{k}_h^2\mathbb{I} - 2\gamma_2\sum_{\alpha=x,y,z}J_\alpha^2\left(\hat{k}_{\alpha h}^2 - \frac{1}{3}\hat{k}_h^2\right)\right.\\ &\left. - 4\gamma_3\sum_{\alpha\neq\beta}\{J_\alpha, J_\beta\}\hat{k}_{\alpha h}\hat{k}_{\beta h}\right].\end{aligned} \tag{A.1}$$

Here $\hat{k}_e$ and $\hat{k}_h$ are the operators of the wave vectors of a free electron and hole. The remaining notations used in this Appendix are explained in Section 1.

The coordinates of a free electron and hole can be transformed into those for the exciton center of mass and relative electron–hole motion according to the expressions; see, e.g., [51]

$$\mathbf{R} = \frac{\mathbf{r}_e m_e + m_h\mathbf{r}_h}{m_e + m_h},\ \mathbf{r} = \mathbf{r}_h - \mathbf{r}_e. \tag{A.2}$$

Under the conditions we considered in Section 1, the operators of free electron and hole can be expressed in terms of the momentum operator of relative motion and the wave vector of exciton motion, see, e.g., [51]

$$\begin{aligned}\hat{k}_{zh} &= \frac{m_h}{m_e+m_h}K + \frac{1}{\hbar}\hat{p}_z + \frac{e}{c\hbar}\frac{m_e}{m_e+m_h}A_z,\\ \hat{k}_{x,yh} &= \frac{1}{\hbar}\hat{p}_{x,y} + \frac{e}{c\hbar}\frac{m_e}{m_e+m_h}A_{x,y},\\ \hat{k}_{ze} &= \frac{m_e}{m_e+m_h}K - \frac{1}{\hbar}\hat{p}_z + \frac{e}{c\hbar}\frac{m_h}{m_e+m_h}A_z,\\ \hat{k}_{x,ye} &= -\frac{1}{\hbar}\hat{p}_{x,y} + \frac{e}{c\hbar}\frac{m_h}{m_e+m_h}A_{x,y}.\end{aligned} \tag{A.3}$$

Substituting these expressions into (A.1) and taking into account Eqs. (2) and (A.2), we obtain

$$\begin{aligned}\hat{\mathbb{H}}_X &= \mathbb{L}\frac{\hbar^2K^2}{2} - \frac{\hat{p}^2}{2\mu} - \frac{e^2}{\epsilon_0 r} + \left(\frac{e}{c}\right)\mathbb{L}\hbar KA_z\\ &- 2\frac{\gamma_3}{m_0}\left(\frac{e}{c}\right)\frac{m_e m_h}{(m_e+m_h)^2}\left(\{J_x, J_z\}KA_x + \{J_y, J_z\}KA_y\right)\\ &+ \left(\frac{e}{c}\right)^2\frac{m_e^3+m_h^3}{2(m_e+m_h)^2 m_e m_h}\sum_{\alpha=x,y,z}A_\alpha^2.\end{aligned} \tag{A.4}$$

The components of the vector potential of the magnetic field $A_{x,y,z}$ are specified ambiguously, and their form depends on the gauge. The most convenient for calculations is Landau gauge (3). This gauge corresponds to a new Cartesian coordinate system, in which the field is still directed along $x \parallel [100]$, and the y' axis is chosen parallel to the Lorentz force vector. At $\mathbf{B} \parallel [100]$, the y'-axis is directed along [011], and z' along $[0\bar{1}1]$.

The transformation into a new coordinate system with taking into account the gauge (3) results in the following replacements in the expression (A.4): $K_z \to \sqrt{K_{y'}^2 + K_{z'}^2}$, where $K_{y'} = K/\sqrt{2}$ and $K_{z'} = K/\sqrt{2}$; $A_z \to A_{y'}/\sqrt{2}$, $A_y \to A_{y'}/\sqrt{2}$, $A_x \to 0$; $\hat{p}^2 \to (\hat{p}')^2$, and $r \to r'$. After this transformation, we can omit the primes in superscript of the new coordinates and obtain the Hamiltonian (4).

Appendix B

To obtain a numerical solution of the eigenvalue problem with a Hamiltonian (6), we employ the finite-difference approximation of the operators (7), see, e.g., [62]. First, we consider the cylindrical coordinates as discrete values: $y = hj$ and $\rho = hu$. Here h is the grid step, and j and u are integers from 1 to N for states characterized by angular momenta projections of electron and hole $|3/2, -1/2\rangle$ and from $N+1$ to $2N$ for states with angular momenta projections $|1/2, -1/2\rangle$.

The second derivative operators are represented by the central second-order finite-difference formulas

$$\begin{aligned}\frac{\partial^2\varphi^{(\alpha)}(y,\rho)}{\partial\rho^2} &= \frac{\varphi_{j,u+1}^{(\alpha)} - 2\varphi_{ju}^{(\alpha)} + \varphi_{j,u-1}^{(\alpha)}}{h^2} + O(h^2),\\ \frac{\partial^2\varphi^{(\alpha)}(y,\rho)}{\partial y^2} &= \frac{\varphi_{j+1,u}^{(\alpha)} - 2\varphi_{ju}^{(\alpha)} + \varphi_{j-1,u}^{(\alpha)}}{h^2} + O(h^2).\end{aligned} \tag{B.1}$$

Here, values $\varphi_{j,u}^{\alpha}$ are the unknown quantities of the eigenfunction on the coordinate grid. The index $\alpha = |3/2, -1/2\rangle$ or $|1/2, -1/2\rangle$.

Also, the expressions (7) include the first derivative with respect to ρ, which can be represented as

$$\frac{\partial\varphi^{(\alpha)}(y,\rho)}{\partial\rho} = \frac{\varphi_{j,u+1}^{(\alpha)} - \varphi_{j,u-1}^{(\alpha)}}{2h} + O(h^2). \tag{B.2}$$

The operator $\hat{V}_{KB}$ in the expression (7) describing the mixing between the states $|3/2, -1/2\rangle$ and $|1/2, -1/2\rangle$ is represented

$$\hat{V}_{KB}\varphi^{(\alpha)}(y,\rho) = \beta KB\varphi_{j\pm N,u\pm N}^{(\alpha)}jh, \tag{B.3}$$

where the upper sign of the index corresponds to $\alpha = |3/2, -1/2\rangle$, and the lower sign to $\alpha = |1/2, -1/2\rangle$.

The remaining terms in the expression (7) should be transformed using the replacements $y = hj$ and $\rho = hu$. At given magnitudes B and K, these terms are the product of the values $\varphi_{j,u}$ by some constants.

The matrix operator (6) with elements (7) can be represented using finite-difference schemes (B.1)–(B.3) as a some-diagonal matrix. The number of diagonals is equal to the number of quantities of the eigenfunction, which are used to describe the Hamiltonian (6) at given j and u. It is seen from (B.1)–(B.3) that there are only seven such quantities: $\varphi_{j,u}^{\alpha}$, $\varphi_{j\pm1,u}^{\alpha}$, $\varphi_{j,u\pm1}^{\alpha}$, $\varphi_{j\pm N,u\pm N}^{\alpha}$. Thus, the problem of finding the eigenvalues of the Hamiltonian (6) is reduced to the diagonalization of a seven-diagonal matrix.

Data availability

The authors are unable or have chosen not to specify which data has been used.

References

[1] E.L. Ivchenko, Optical Spectroscopy of Semiconductor Nanotstructures, Alpha Science, Harrow, 2005.
[2] A.V. Kavokin, J.J. Baumberg, G. Malpuech, F.P. Laussy, Microcavities, Oxford University, New York, 2007.
[3] C.F. Klingshirn, Semiconductor Optics, fourth ed., Springer, Berlin, 2012.
[4] N. Tomassini, A. D'Andrea, R. Del Sole, H. Tuffigo-Ulmer, R.T. Cox, Center-of-mass quantization of excitons in $CdTe/Cd_{1-x}Zn_xTe$ quantum wells, Phys. Rev. B 51 (1995) 5005.
[5] E.S. Khramtsov, P.A. Belov, P.S. Grigoryev, I.V. Ignatiev, S.Yu. Verbin, Yu.P. Efimov, S.A. Eliseev, V.A. Lovtcius, V.V. Petrov, S.L. Yakovlev, Radiative decay rate of excitons in square quantum wells: Microscopic modeling and experiment, J. Appl. Phys. 119 (2016) 184301.
[6] A. Tredicucci, Y. Chen, F. Bassani, J. Massies, C. Deparis, G. Neu, Center-of-mass quantization of excitons and polariton interference in GaAs thin layers, Phys. Rev. B 47 (1993) 10348.
[7] H.C. Schneider, F. Jahnke, S.W. Koch, J. Tignon, T. Hasche, D.S. Chemla, Polariton propagation in high quality semiconductors: Microscopic theory and experiment versus additional boundary conditions, Phys. Rev. B 63 (2001) 045202.

[8] G. Göger, M. Betz, A. Leitenstorfer, M. Bichler, W. Wegscheider, G. Abstreiter, Ultrafast optical spectroscopy of large-momentum excitons in GaAs, Phys. Rev. Lett. 84 (2000) 5812.

[9] M. Betz, G. Göger, A. Leitenstorfer, M. Bichler, G. Abstreiter, W. Wegscheider, Nonlinear optical response of highly energetic excitons in GaAs: Microscopic electrodynamics at semiconductor interfaces, Phys. Rev. B 65 (2002) 085314.

[10] E.V. Ubyivovk, Yu.K. Dolgikhand Yu.P. Efimov, S.A. Eliseev, I.Ya. Gerlovin, I.V. Ignatiev, V.V. Petrov, V.V. Ovsyankin, Spectroscopy of high-energy excitonic states in ultra-thick GaAs quantum wells with a perfect crystal structure, J. Lum. 751 (2003) 102–103.

[11] E.V. Ubyivovk, D.K. Loginov, I.Ya. Gerlovin, Yu.K. Dolgikhand Yu.P. Efimov, S.A. Eliseev, V.V. Petrov, O.F. Vyvenko, A.A. Sitnikova, D.A. Kirilenko, Experimental determination of dead layer thickness for excitons in a wide GaAs/AlGaAs quantum well, Fiz. Tverd. Tela 51 (2009) 1818;
Phys. Solid State 51 (2009) 1929.

[12] D. Schiumarini, N. Tomassini, L. Pilozzi, A. D'Andrea, Polariton propagation in weak-confinement quantum wells, Phys. Rev. B 82 (2010) 075303.

[13] E.S. Khramtsov, P.S. Grigoryev, D.K. Loginov, I.V. Ignatiev, Yu.P. Efimov, S.A. Eliseev, P. Yu. Shapochkin, E.L. Ivchenko, M. Bayer, Exciton spectroscopy of optical reflection from wide quantum wells, Phys. Rev. B 99 (2019) 035431.

[14] S. Schumacher, G. Czycholl, F. Jahnke, I. Kudyk, H.I. Rückmann, J. Gutowski, A. Gust, G. Alexe, D. Hommel, Polariton propagation in shallow-confinement heterostructures: Microscopic theory and experiment showing the breakdown of the dead-layer concept, Phys. Rev. B 70 (2004) 235340.

[15] A.V. Trifonov, S.N. Korotan, A.S. Kurdyubov, I.Ya. Gerlovin, I.V. Ignatiev, Yu.P. Efimov, S.A. Eliseev, V.V. Petrov, V.V. Yu.K. Dolgikhand Ovsyankin, A.V. Kavokin, Nontrivial relaxation dynamics of excitons in high-quality InGaAs/GaAs quantum wells, Phys. Rev. B 91 (2015) 115307.

[16] M. Nakayama, D. Kim, H. Ishihara, Center-of-mass quantization of excitons in PbI_2 thin films grown by vacuum deposition, Phys. Rev. B 74 (2006) 073306.

[17] D.K. Loginov, A.V. Trifonov, I.V. Ignatiev, Effect of uniaxial stress on the interference of polaritonic waves in wide quantum wells, Phys. Rev. B 90 (2014) 075306.

[18] D.K. Loginov, P.S. Grigoryev, Yu.P. Efimov, S.A. Eliseev, V.A. Lovtcius, V.V. Petrov, E.V. Ubyivovk, I.V. Ignatiev, Reduction of exciton mass by uniaxial stress in GaAs/AlGaAs quantum wells, Phys. Stat. Sol. B 253 (2016) 1537.

[19] S. Zielinska-Raczynska, D. Ziemkiewicz, G. Czajkowski, Electro-optical properties of Cu_2O for P excitons in the regime of Franz-Keldysh oscillations, Phys. Rev. B 97 (2018) 165205.

[20] D.K. Loginov, P.A. Belov, V.G. Davydov, I.Ya. Gerlovin, I.V. Ignatiev, A.V. Kavokin, Y. Masumoto, Exciton-polariton interference controlled by electric field, Phys. Rev. Res. 2 (2020) 033510.

[21] R. Kotlyar, T.L. Reinecke, M. Bayer, A. Forchel, Zeeman spin splittings in semiconductor nanostructures, Phys. Rev. B 63 (2001) 085310.

[22] Y.H. Chen, X.L. Ye, B. Xu, Z.G. Wang, Z. Yang, Large g factors of higher-lying excitons detected with reflectance difference spectroscopy in GaAs-based quantum wells, Appl. Phys. Lett. 89 (2006) 051903.

[23] J.J. Davies, D. Wolverson, V.P. Kochereshko, A.V. Platonov, R.T. Cox, J. Cibert, H. Mariette, C. Bodin, C. Gourgon, E.V. Ubyivovk, Yu.P. Efimov, S.A. Eliseev, Motional enhancement of exciton magnetic moments in zinc-blende semiconductors, Phys. Rev. Lett. 97 (2006) 187403.

[24] A. Litvinov, V.P. Kochereshko, D. Loginov, L. Besombes, H. Mariette, J.J. Davies, L.C. Smith, D. Wolverson, Motional enhancement of exciton magnetic moments, Acta Phys. Pol. A 112 (2007) 161.

[25] J. Jadczak, M. Kubisa, K. Ryczko, L. Bryja, M. Potemski, High magnetic field spin splitting of excitons in asymmetric GaAs quantum wells, Phys. Rev. B 86 (2012) 245401.

[26] A. Arora, A. Mandal, S. Chakrabarti, S. Ghosh, Magneto-optical Kerr effect spectroscopy based study of Lande g-factor for holes in GaAs/AlGaAs single quantum wells under low magnetic fields, J. Appl. Phys. 113 (2013) 213505.

[27] W. Bardyszewski, S.P. Lepkowski, Nonlinear Zeeman splitting of magnetoexcitons in c-plane wurtzite GaN-based quantum wells, Phys. Rev. B 90 (2014) 075302.

[28] P.S. Grigoryev, O.A. Yugov, S.A. Eliseev, Yu.P. Efimov, V.A. Lovtcius, V.V. Petrov, V.F. Sapega, I.V. Ignatiev, Inversion of Zeeman splitting of exciton states in InGaAs quantum wells, Phys. Rev. B 93 (2016) 205425.

[29] L.V. Butov, C.W. Lai, D.S. Chemla, Yu.E. Lozovik, K.L. Campman, A.C. Gossard, Observation of magnetically induced effective-mass enhancement of quasi-2D excitons, Phys. Rev. Lett. 87 (2001) 216804.

[30] Yu. E. Lozovik, I.V. Ovchinnikov, S. Yu. Volkov, L.V. Butov, D.S. Chemla, Quasi-two-dimensional excitons in finite magnetic fields, Phys. Rev. B 65 (2002) 235304.

[31] D.Loginov V.P. Kochereshko, A. Litvinov, L. Besombes, H. Mariette, J.J. Davies, L.C. Smith, D. Wolverson, Excitonic polaritons in transverse magnetic fields, Acta Phys. Pol. A 112 (2007) 381.

[32] L.C. Smith, J.J. Davies, D. Wolverson, S. Crampin, R.T. Cox, J. Cibert, H. Mariette, V.P. Kochereshko, M. Wiater, G. Karczewski, T. Wojtowicz, Motion-dependent magnetic properties of excitons in CdTe, Phys. Rev. B 78 (2008) 085204.

[33] J. Wilkes, E.A. Muljarov, Exciton effective mass enhancement in coupled quantum wells in electric and magnetic fields, New J. Phys. 18 (2016) 023032.

[34] S. Yu. Bodnar, P.S. Grigoryev, D.K. Loginov, V.G. Davydov, Yu.P. Efimov, S.A. Eliseev, V.A. Lovtcius, E.V. Ubyivovk, V.Yu. Mikhailovskii, I.V. Ignatiev, Exciton mass increase in a GaAs/AlGaAs quantum well in a transverse magnetic field, Phys. Rev. B 95 (2017) 195311.

[35] A. Chaves, F.M. Peeters, Tunable effective masses of magneto-excitons in two-dimensional materials, Solid. State Com. 1143 (2021) 334–33571.

[36] P.S. Grigoryev, M.A. Chukeev, V.A. Lovtcius, Yu.P. Efimov, S.A. Eliseev, Zeeman splitting of excitons in GaAs/AlGaAs quantum wells in the Faraday geometry, JETP 137 (2023) 656.

[37] A.G. Samoilovich, L.L. Korenblit, Magneto-optical properties of the exciton, Dokl. Akad. Nauk SSSR 100 (1955) 43.

[38] D.G. Thomas, J.J. Hopfield, Direct observation of exciton motion in CdS, Phys. Rev. Lett. 5 (1960) 505.

[39] E.F. Gross, B.P. Zakharchenya, O.V. Konstantinov, Effect of magnetic field inversion in spectra of exciton absorption in CdSe crystal, Fiz. Tverd. Tela 3 (1961) 305;
Sov. Phys.—Solid State 3 (1961) 221.

[40] D.G. Thomas, J.J. Hopfield, A magneto-Stark effect and exciton motion in CdS, Phys. Rev. B 124 (1961) 657.

[41] L.P. Gor'kov, I.E. Dzyaloshinskii, Contribution to the theory of the Mott exciton in a strong magnetic field, Zh. Eksp. Teor. Fiz. 53 (1967) 717;
JETP 26 (1968) 449.

[42] B.S. Monozon, P. Schmelcher, Optical absorption by excitons in semiconductor quantum wells in tilted magnetic and electric fields, Phys. Rev. B 82 (2010) 205313.

[43] M. Lafrentz, D. Brunne, B. Kaminski, V.V. Pavlov, A.V. Rodina, R.V. Pisarev, D.R. Yakovlev, A. Bakin, M. Bayer, Magneto-Stark effect of excitons as the origin of second harmonic generation in ZnO, Phys. Rev. Lett. 110 (2013) 116402.

[44] M. Lafrentz, D. Brunne, A.V. Rodina, V.V. Pavlov, R.V. Pisarev, D.R. Yakovlev, A. Bakin, M. Bayer, Second-harmonic generation spectroscopy of excitons in ZnO, Phys. Rev. B 88 (2013) 235207.

[45] A. Farenbruch, J. Mund, D. Fröhlich, D.R. Yakovlev, M. Bayer, M.A. Semina, M.M. Glazov, Magneto-Stark and Zeeman effect as origin of second harmonic generation of excitons in Cu_2O, Phys. Rev. B 101 (2020) 115201.

[46] Patric Rommel, Jörg Main, Andreas Farenbruch, Johannes Mund, Dietmar Fröhlich, Dmitri R. Yakovlev, Manfred Bayer, Christoph Uihlein, Second harmonic generation of cuprous oxide in magnetic fields, Phys. Rev. B 101 (2020) 115202.

[47] I.Y. Chestnov, S.M. Arakelian, A.V. Kavokin, Giant synthetic gauge field for spinless microcavity polaritons in crossed electric and magnetic fields, New J. Phys. 23 (2021) 023024.

[48] Todd Karin, Xiayu Linpeng, M.M. Glazov, M.V. Durnev, E.L. Ivchenko, Sarah Harvey, Ashish K. Rai, Arne Ludwig, Andreas D. Wieck, Kai-Mei C. Fu, Giant permanent dipole moment of two-dimensional excitons bound to a single stacking fault, Phys. Rev. B 94 (2016) 041201(R).

[49] P. Andreakou, A.V. Mikhailov, S. Cronenberger, D. Scalbert, A. Nalitov, A.V. Kavokin, M. Nawrocki, L.V. Butov, K.L. Campman, A.C. Gossard, M. Vladimirova, Influence of magnetic quantum confined Stark effect on the spin lifetime of indirect excitons, Phys. Rev. B 93 (2016) 115410.

[50] Mikhail V. Durnev, Mikhail M. Glazov, Xiayu Linpeng, Maria L.K. Viitaniemi, Bethany Matthews, Steven R. Spurgeon, Peter V. Sushko, Andreas D. Wieck, Arne Ludwig, Kai-Mei C. Fu, Microscopic model for the stacking-fault potential and the exciton wave function in GaAs, Phys. Rev. B 101 (2020) 125420.

[51] K. Cho, S. Suga, W. Dreybrodt, F. Willmann, Theory of degenerate $1s$ excitons in zinc-blende-type crystals in a magnetic field: Exchange interaction and cubic anisotropy, Phys. Rev. B 11 (1975) 1512.

[52] L.D. Landau, E.M. Lifshitz, Quantum Mechanics, Course of Theoretical Physics, vol. 3, third ed., Pergamon, New York, 1999, p. 456.

[53] Evan O. Kane, Exciton dispersion in degenerate bands, Phys. Rev. B 11 (1975) 3850.

[54] E.L. Ivchenko, G. Pikus, Superlattices and Other Microstructures, Springer-Verlag, Berlin, 1995.

[55] W. Dreybrodt, F. Willmann, M. Bettini, E. Bauser, Energy of free and bound excitons in GaAs in a magnetic field, Solid State Commun. 12 (1973) 1217.

[56] S.B. Nam, D.C. Reynolds, C.W. Litton, R.J. Almassy, T.C. Collins, C.M. Wolfe, Free-exciton energy spectrum in GaAs, Phys. Rev. B 13 (1976) 761.

[57] V.P. Dolgopolskii, R.P. Seisyan, A.L. Efros Jr., The ground state of a wannier-mott exciton in diamond-like semiconductors in intermediate magnetic fields, Phys. Stat. Sol. B 88 (1978) K177.

[58] T.M. Rusin, The energy of excitons in parabolic quantum wells investigated by the effective variational Hamiltonian method, J. Phys.: Condens. Matter. 12 (2000) 575.

[59] J. Wilkes, E.A. Muljarov, Exciton effective mass enhancement in coupled quantum wells in electric and magnetic fields, New J. Phys. 18 (2016) 023032.

[60] A. Jaeger, G. Weiser, Excitonic electroabsorption spectra and Franz-Keldysh effect of $In_{0.53}Ga_{0.47}As/InP$ studied by small modulation of static fields, Phys. Rev. B 58 (1998) 10674.

[61] Sten Haastrup, Simone Latini, Kirill Bolotin, Kristian S. Thygesen, Stark shift and electric-field-induced dissociation of excitons in monolayer MoS_2 and hBN/MoS_2 heterostructures, Phys. Rev. B 94 (2016) 041401(R).

[62] A.A. Samarskii, The Theory of Difference Schemes, Pure and Applied Mathematics, in: A Series of Monographs and Textbooks, CRC Press, Boca Raton, FL, 2001.
[63] I. Vurgaftman, J.R. Meyer, L.R. Ram-Mohan, Band parameters for III-V compound semiconductors and their alloys, J. Appl. Phys. 89 (2001) 5815.
[64] G.E. Stillman, D.M. Larsen, C.M. Wolfe, R.C. Brandt, Precision verification of effective mass theory for shallow donors in GaAs, Solid State Commun. 9 (1971) 2245.
[65] A. Frova, P. Handler, F.A. Germano, D.E. Aspnes, Electro-absorption effects at the band edges of silicon and germanium, Phys. Rev. 145 (1966) 575.
[66] D.F. Blossey, Wannier exciton in an electric field. I. Optical absorption by bound and continuum states, Phys. Rev. B 2 (1970) 3976.